International Journal of Pharmaceutics 569 (2019) 118563

Contents lists available at ScienceDirect

International Journal of Pharmaceutics

journal homepage: www.elsevier.com/locate/ijpharm

Coloring of PLGA implants to better understand the underlying drug release mechanisms

C. Bode[a], H. Kranz[b], F. Siepmann[a], J. Siepmann[a,*]

[a] Univ. Lille, Inserm, CHU Lille, U1008, F-59000 Lille, France
[b] Bayer AG, Muellerstraße 178, 13353 Berlin, Germany

ARTICLE INFO

Keywords:
PLGA
Implant
Drug release mechanism
Swelling
Diffusion

ABSTRACT

Different dyes and a colored vitamin (riboflavin) were used to better understand the underlying drug release mechanisms in poly(lactic-co-glycolic acid) (PLGA)-based implants. The latter were prepared by hot melt extrusion (HME) or formed *in-situ*, upon solvent exchange when injecting a PLGA solution in N-methyl-pyrrolidone (NMP) into phosphate buffer pH 7.4. Methylene blue was used as water-soluble dye to stain the release medium, riboflavin as a yellow, water-soluble "model drug", and Sudan-III-red as poorly water-soluble dye, incorporated in the implant. In the case of pre-formed HME implants, the "orchestrating" role of polymer swelling for the control of drug release could be visualized: At early time points, only limited amounts of water penetrate into the system, insufficient for noteworthy drug dissolution and diffusion. However, bulk erosion starts, and once a critical polymer molecular weight threshold value is reached, substantial implant swelling sets on: Large amounts of water come in and allow for significant drug dissolution and diffusion. In the case of *in-situ* forming implants, the importance of the composition of the liquid formulation for the resulting inner implant structure could be visualized. The latter affects the rate and extent at which water penetrates into the system and, thus, the resulting drug release rate.

1. Introduction

Poly(lactic-co-glycolic acid) (PLGA) is frequently used as matrix former in parenteral controlled drug delivery systems (Kranz and Bodmeier, 2007; Lee et al., 2010; Wischke and Schwendeman, 2012; Shah and Schwendeman, 2014; Gonzalez-Pizarro et al., 2018; Bragagni et al., 2018). It provides several major advantages, such as: (i) complete biodegradability (Vert et al., 1994), (ii) biocompatibility (Anderson and Shive, 1997; Fournier et al., 2003), and (iii) the possibility to control drug release during flexible periods of time, ranging from a few days up to several weeks (Ravivarapu et al., 2000; Klose et al., 2008; Wischke and Schwendeman, 2008; Mylonaki et al., 2018b). Upon hydrolytic chain cleavage, it is degraded into lactic and glycolic acid. For many decades PLGA has been used in bioresorbable sutures (Gilding and Reed, 1979), and for many years several drug products based on PLGA are commercially available. Different types of dosage forms can be prepared using PLGA as release rate controlling excipient, in particular microparticles and implants (Johansen et al., 1998; Berkland et al., 2002; Ibrahim et al., 2005; Zhang and Schwendeman, 2012; Do et al., 2014; Sheikh Hasan et al., 2015; Agossa et al., 2017; Duque et al., 2018).

PLGA-based implants can be prepared using different manufacturing techniques, including for example compression (Astaneh et al., 2008; Wischke and Schwendeman, 2012), hot melt extrusion (HME) (DesNoyer and McHugh, 2003; Wang et al., 2003; Ghalanbor et al., 2012), and *in-situ* formation upon injection of a liquid formulation into living tissue (Hatefi and Amsden, 2002; Kempe et al., 2008; Kranz and Bodmeier, 2008; Kempe and Mäder, 2012; Kamali et al., 2018). In the latter case, for instance solvent exchange can induce implant formation: The PLGA can be dissolved in a water-miscible solvent, such as N-methyl-pyrrolidone (NMP). Upon contact with aqueous body fluids, the NMP diffuses out into the surrounding environment and water diffuses into the formulation. Since PLGA is not soluble in water, it precipitates as soon as a critical NMP/water ratio is reached. The advantage of *in-situ* forming (compared to preformed) implants is that the liquid formulations can generally relatively easily be injected (compared to the implantation of larger preformed devices).

The resulting drug release rate from a PLGA-based drug delivery system depends on various factors, such as the geometry and size of the dosage form (Lin et al., 2018), drug properties (e.g. solubility, affinity to PLGA), composition (e.g. drug loading, presence of potential additives) (Do et al., 2015a; Hamoudi-Ben Yelles et al., 2017; Wu et al.,

* Corresponding author at: University of Lille, College of Pharmacy, Inserm U1008, 3 rue du Professeur Laguesse, 59006 Lille, France.
E-mail address: juergen.siepmann@univ-lille.fr (J. Siepmann).

https://doi.org/10.1016/j.ijpharm.2019.118563
Received 8 June 2019; Received in revised form 22 July 2019; Accepted 23 July 2019
Available online 24 July 2019
0378-5173/

2018), type of PLGA (e.g. differing in the macromolecular chain length or type of end groups) (Mylonaki et al., 2018a), and type of preparation technique (determining the systems' inner structure, and thus, conditions for drug release) (Do et al., 2015b). It has to be pointed out that the underlying mass transport mechanisms controlling drug release in PLGA-based delivery systems might be rather complex (Friess and Schlapp, 2002; Berkland et al., 2007; Kang and Schwendeman, 2007; Fredenberg et al., 2011). For instance, the following phenomena can be involved and might be of importance: water penetration into the dosage form, PLGA precipitation (in the case of *in-situ* forming systems), drug dissolution (Siepmann and Siepmann, 2013), drug diffusion (Siepmann and Siepmann, 2012), polymer chain cleavage, crystallization of degradation products (Gopferich, 1996), system swelling (Gasmi et al., 2016, 2015a,b), autocatalytic effects, and erosion (dry mass loss). Autocatalytic effects might occur, because ester chain cleavage is catalyzed by protons, and short chain acids are generated upon PLGA degradation (Brunner et al., 1999; Fu et al., 2000; Schädlich et al., 2014). Case by case, the importance of such autocatalytic effects depends on the rate at which the short chain acids are generated and at which rate they diffuse out into the surrounding environment, or are neutralized by bases penetrating into the system (Siepmann et al., 2005; Klose et al., 2006). In case of pronounced autocatalytic effects, the dosage form can become more and more hollow with time.

Recently, the crucial role of PLGA swelling (which is often neglected) has been pointed out for the control of dexamethasone release from HME implants (Bode et al., 2019): Briefly, it has been shown that the amounts of water penetrating into the systems are limited at early time points, not enabling noteworthy drug dissolution and diffusion. Thus, during a certain time period ("lag time") dexamethasone release was negligible (the implants' surface was not porous in this case). However, the limited amounts of water, which did penetrate into the implants right upon exposure to the aqueous release medium, started polymer chain cleavage throughout the systems ("bulk erosion"). With decreasing polymer molecular weight, the PLGA chains became more and more hydrophilic and less entangled. In addition, water-soluble degradation products generated a steadily increasing osmotic pressure within the implants. As soon as a certain molecular weight threshold value was reached, substantial amounts of water came in and allowed for significant drug dissolution and diffusion: drug release set on. However, only limited information is yet available on potential structural changes within PLGA-based implants during drug release. The use of dyes and colored "model drugs" might help overcoming this lack.

The aim of this study was to use different types of dyes and a colored vitamin to get further insight into the underlying mass transport mechanisms from PLGA-based implants. Methylene blue was used as water-soluble dye to stain the release medium. Riboflavin was selected as water-soluble, colored vitamin and incorporated into the implants. And Sudan-III-red was chosen as poorly water-soluble dye and also incorporated into different types of PLGA-based implants. The latter were prepared by hot melt extrusion (HME) or formed *in-situ*, upon injection of a PLGA solution in NMP into phosphate buffer pH 7.4.

2. Materials and methods

2.1. Materials

Poly(D,L-lactic-co-glycolic acid) (50:50, –COOH end groups, PLGA, Resomer RG 502 H; Evonik, Darmstadt, Germany); riboflavin (DSM Nutritional Products, Basel, Switzerland); Sudan-III-red (Merck, Darmstadt, Germany); methylene blue (Sigma Aldrich, Steinheim, Germany); polyoxyethylene glycol sorbitan monooleate (Tween 80; Cooper, Melun, France); N-methyl-pyrrolidone (NMP) and acetonitrile (Fisher Scientific, Illkirch, France); ethanol 96% (VWR, Fontenay-sous-Bois, France); formic acid (Riedel-de Haen, Seelze, Germany).

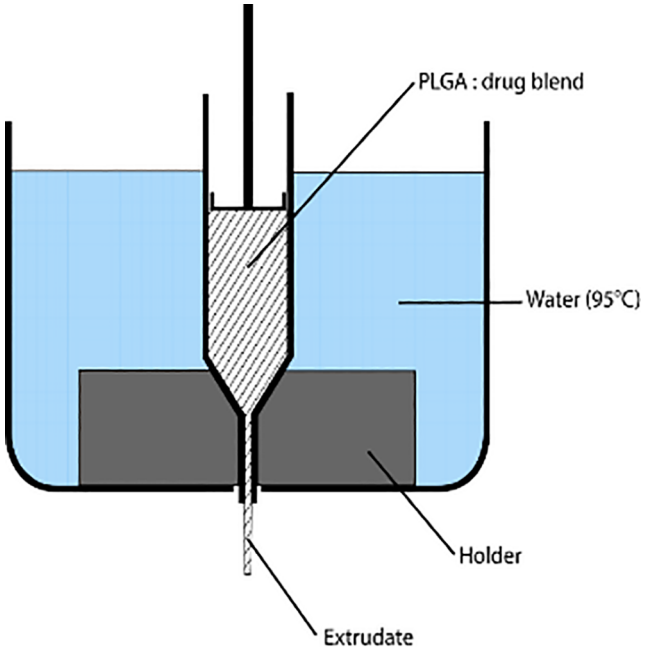

Fig. 1. Set-up used to prepare dexamethasone implants by hot melt extrusion (reproduced from Bode et al., 2019, with permission).

2.2. Implant preparation

Hot melt extrusion (HME): Poly(lactic-co-glycolic acid) (PLGA Resomer RG 502H) and 1% riboflavin or Sudan-III-red were mixed for 5 min at 98 rpm in a Turbula Shaker-Mixer (T2A; Willy A. Bachofen, Basel, Switzerland), followed by 5 min manual blending with a mortar and pestle to ensure a homogenous blend. The mixtures were filled into 5 mL syringes, equipped with a shortened 16G needle (1.5 cm). Fig. 1 shows schematically the set-up used to prepare the implants by hot melt extrusion. The syringe was fixed in a holder. A water bath kept the temperature at 95 °C. After 5 min, the content of the syringe was molten, and a texture analyzer (TAXT plus, 50 kg loading cell; Stable Micro Systems, Surrey, UK) was used to drive the syringe plunger downwards at a speed of 0.6 mm/min. The obtained extrudates were manually cut into cylinders of approximately 5 mm length, using a heated blade.

In-situ forming implants: Appropriate amounts of PLGA (Resomer RG 502H) and riboflavin or Sudan-III-red were dissolved in NMP in glass vials under stirring at 500 rpm (Multipoint Stirrer, Thermo Scientific, Loughborough, UK) at room temperature for 60 min. Afterwards, the vials were kept without stirring for 1 h at room temperature to remove air bubbles. The formulations were stored at 2–8 °C, and allowed to reach room temperature prior to use. Eppendorf vials were filled with 4 mL: (i) phosphate buffer pH 7.4 (USP 40) in the case of riboflavin, (ii) phosphate buffer pH 7.4 (USP 40) containing 0.02% Tween 80 in the case of Sudan-III-red, or (iii) phosphate buffer pH 7.4 (USP 40) containing 0.01% methylene blue in the case of vitamin/dye-free implants. All vials were pre-heated overnight at 37 °C. One hundred µL of the liquid PLGA/vitamin/dye/NMP formulations were injected into the vials using a syringe pump (2 mL/min; PHD 2000; Harvard Apparatus, Holliston, USA). Solvent exchange initiated polymer precipitation and *in-situ* implant formation. The Eppendorf vials were placed into a horizontal shaker (80 rpm, 37 °C; GFL 3033, Gesellschaft fuer Labortechnik, Burgwedel, Germany).

2.3. Implant characterization

In vitro vitamin/dye release from HME implants: One implant was placed in 1 Eppendorf vial, filled with 4 mL pre-heated phosphate

buffer pH 7.4 (USP 40) in the case of riboflavin, or 4 mL pre-heated phosphate buffer pH 7.4 (USP 40) containing 0.02% Tween 80 in the case of Sudan-III-red. At determined time points, the release medium was completely renewed. The amount of riboflavin in the withdrawn bulk fluid was determined by HPLC-UV analysis, using a Thermo Fisher Scientific Ultimate 3000 Series HPLC, equipped with a LPG 3400 SD/RS pump, an auto sampler (WPS-3000 SL) and a UV–Vis detector (VWD-3400RS) (Thermo Fisher Scientific, Waltham, USA). Samples were centrifuged for 2.5 min at 10,000 rpm (Centrifuge Universal 320; Hettich, Tuttlingen, Germany), and filtered with a 0.45 µm PVDF syringe filter (Millex-HV, Merck Millipore, Tullagreen, Ireland). Ten µL samples were injected into a polar C18 column (Luna Omega 3 µm Polar C18 100 Å, 150 mm × 4.6 mm; Phenomenex, Le Pecq, France). The mobile phase consisted of a 85:15 (v/v) mixture of a 0.1% formic acid solution and acetonitrile, the flow rate was 0.8 mL/min. Riboflavin had a retention time of approximately 6.8 min, the detection wavelength was $\lambda = 270$ nm. The calibration curve was linear ($R > 0.999$) within the range of 0.06–0.00004 mg/mL. To determine the amount of riboflavin potentially remaining in the implants at the end of the observation period, the remnants were freeze-dried for 3 d (Christ Epsilon 2–4 LSC; Martin Christ, Osterode, Germany). The lyophilisates were dissolved in a 4:1 (v/v) mixture of acetonitrile and ethanol. The solutions were filtered using 0.45 µm PVDF filter syringes and analyzed for their riboflavin contents by HPLC-UV (as described above). In all cases, in vitro vitamin release was complete at the end of the observation period in this study and no remaining riboflavin amounts were detected in the implant remnants. All experiments were conducted in triplicate. Mean values ± standard deviations are reported. In the case of Sudan-III-red, dye release was followed visually (the released amounts of dye could not be quantified reliably by HPLC-UV): At pre-determined time points, implant samples were withdrawn, freeze-dried for 3 d (Christ Epsilon 2–4 LSC), and cross-sections observed with an optical image analysis system (Nikon SMZ-U; Nikon, Tokyo, Japan), equipped with a Zeiss camera (AxioCam ICc1; Zeiss, Jena, Germany). The cross-sections were obtained by cutting with a heated blade in the case of HME implants, and by manual breaking in the case of *in-situ* forming implants. In vitro vitamin/dye release from *in-situ* forming implants was measured in the same way (the implants were formed in the Eppendorf vials used for the in vitro release studies).

Implant swelling: Implants were treated as for the in vitro release studies. At pre-determined time points, implant samples were withdrawn, excess water carefully removed using Kimtech precision wipes (Kimberly-Clark, Rouen, France) and weighed [*wet mass (t)*]. The *wet mass (%) (t)* was calculated as follows:

$$wet\ mass\ (\%)\ (t) = \frac{wet\ mass\ (t)}{initial\ weight} \times 100\% \quad (1)$$

where *initial weight* is the weight of the pre-formed implant in the case of HME implants, or the total mass of the liquid formulation (PLGA + vitamin/dye + NMP) in the case of *in-situ* forming implants. All experiments were conducted in triplicate. Mean values ± standard deviations are reported.

Implant morphology: Implants were treated as for the in vitro release studies. At pre-determined time points, implants were withdrawn and freeze-dried for 3 d (Christ Epsilon 2–4 LSC). Pictures were taken with an optical image analysis system (Nikon SMZ-U), equipped with a Zeiss camera (AxioCam ICc1). Cross-sections were obtained by cutting (with a heated blade) in the case of HME implants, and by manual breaking in the case of *in-situ* formed implants.

2.4. Determination of the solubility of riboflavin

The solubility of riboflavin (as received) in phosphate buffer pH 7.4 at 37 °C was determined in agitated glass flasks. An excess amount of riboflavin powder (approximately 30 mg) was exposed to 80 mL bulk fluid, kept at 37 °C, under horizontal shaking (80 rpm; GFL 3033).

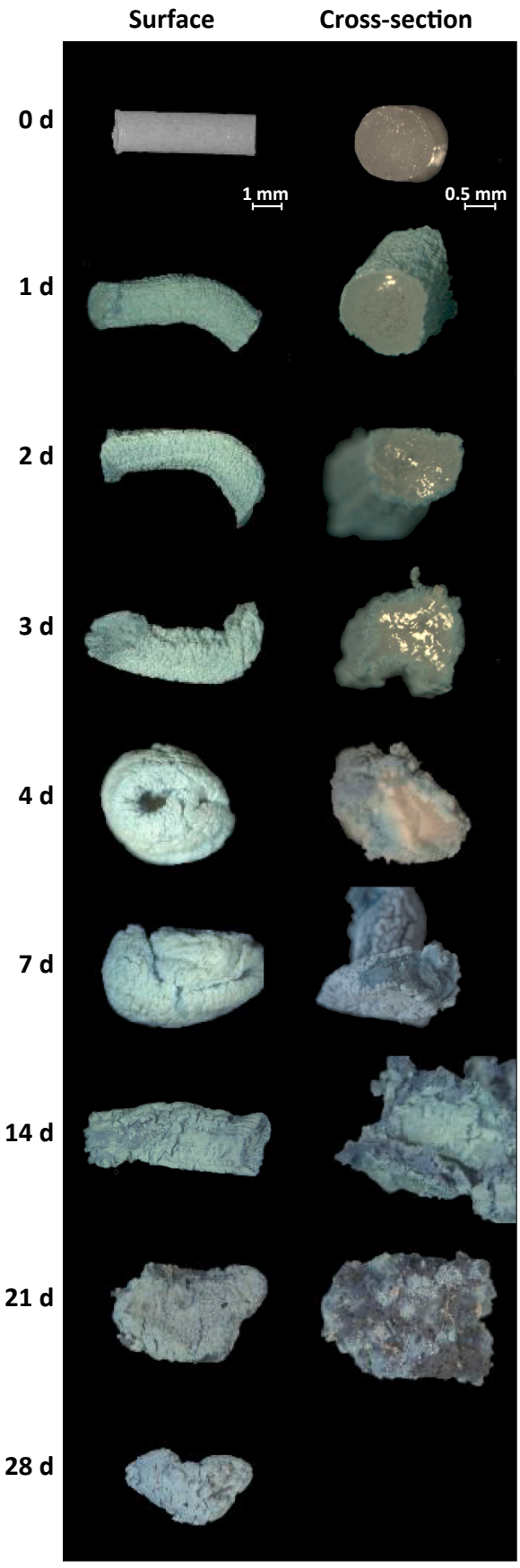

(caption on next page)

Fig. 2. Macroscopic pictures of HME implants (initially vitamin/dye-free) upon exposure to a 0.01% methylene blue solution in phosphate buffer pH 7.4 for different time periods (as indicated), and subsequent freeze-drying. Surfaces are shown on the left hand side, cross-sections on the right hand side. (For interpretation of the references to color in this figure legend, the reader is referred to the web version of this article.)

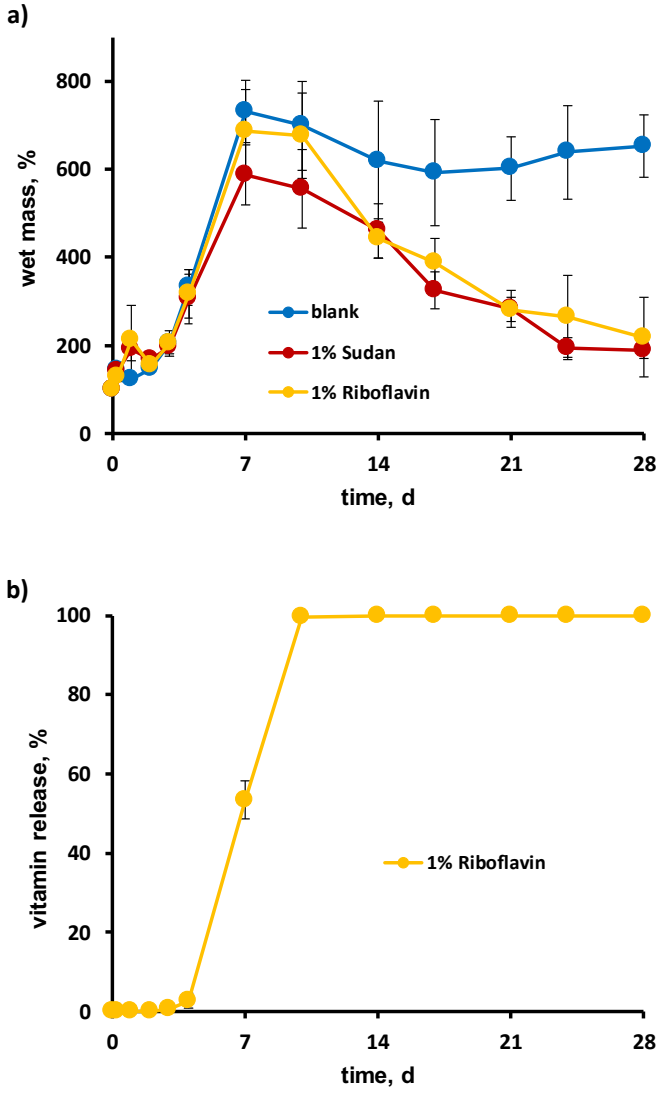

Fig. 3. a) Dynamic changes in the wet mass of HME implants (blank, or loaded with 1% riboflavin or Sudan-III-red, as indicated), upon exposure to the aqueous bulk fluids. b) Riboflavin release from HME implants (1% drug loading) in phosphate buffer pH 7.4. Mean values ± standard deviation are indicated (n = 3). (For interpretation of the references to color in this figure legend, the reader is referred to the web version of this article.)

Samples were withdrawn, immediately filtered (0.45 µm PVDF syringe filter), diluted and analyzed for their riboflavin content by HPLC-UV (as described above, using an injection volume of 20 µL) until equilibrium was reached. Each experiment was conducted in triplicate. Mean values ± standard deviations are reported.

3. Results and discussion

3.1. Pre-formed (HME) implants

Fig. 2 shows macroscopic pictures of PLGA implants prepared by hot melt extrusion (HME), before and after exposure to a 0.01% methylene blue solution in phosphate buffer pH 7.4. Surfaces are shown on the left hand side, cross-sections (obtained by cutting with a heated blade) on the right hand side. The implants were initially vitamin- and dye-free (opaque cylinders, top row). After exposure to the bulk fluid at 37 °C, the implants were removed at pre-determined time points (as indicated) and freeze-dried. Note that this latter step at least partially alters the morphology of the systems. Thus, some caution needs to be paid when drawing conclusions based on these pictures. However, it can clearly be seen that the blue dye progressively penetrated into the implants.

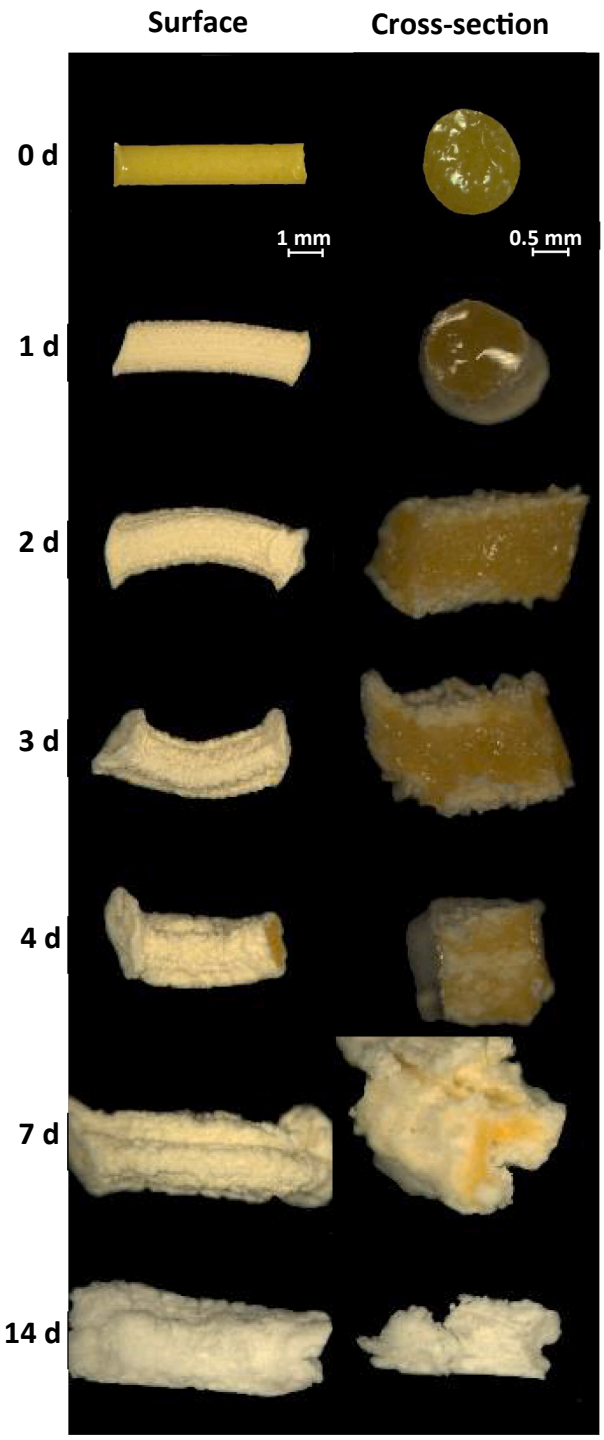

Fig. 4. Macroscopic pictures of HME implants loaded with 1% riboflavin upon exposure to phosphate buffer pH 7.4 for different time periods (as indicated), and subsequent freeze-drying. Surfaces are shown on the left hand side, cross-sections on the right hand side.

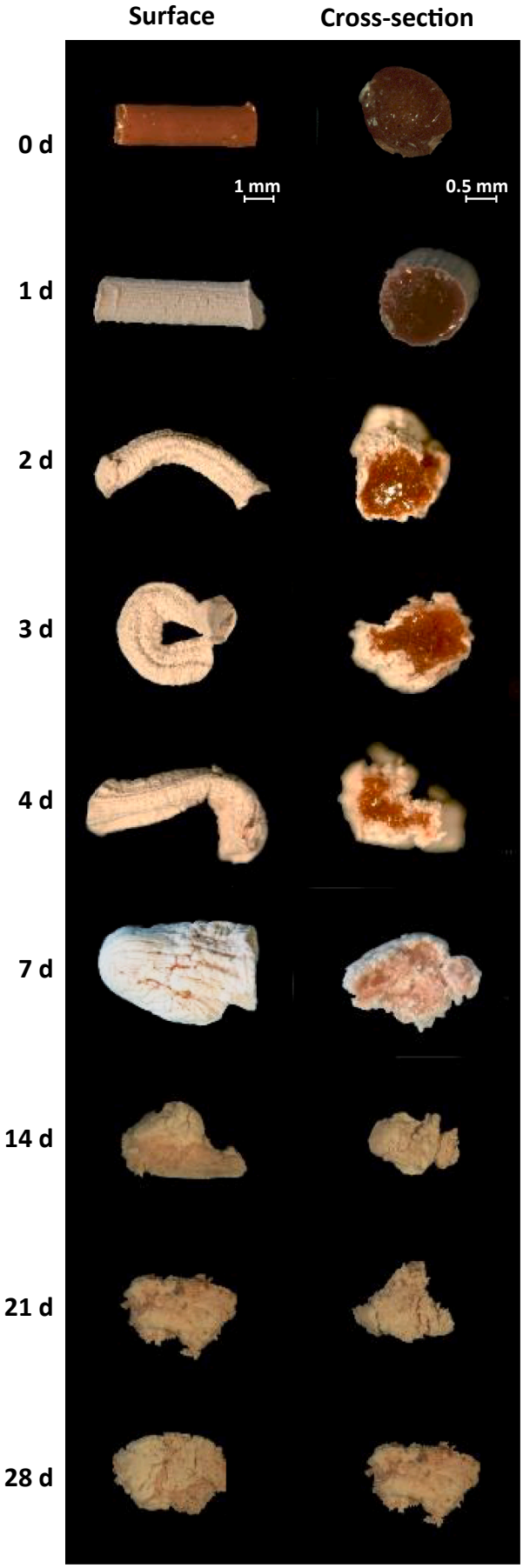

Fig. 5. Macroscopic pictures of HME implants loaded with 1% Sudan-III-red upon exposure to phosphate buffer pH 7.4 (containing 0.02% Tween 80) for different time periods (as indicated), and subsequent freeze-drying. Surfaces are shown on the left hand side, cross-sections on the right hand side. (For interpretation of the references to color in this figure legend, the reader is referred to the web version of this article.)

Importantly, its molecular weight is much higher than that of water (320 vs. 18 Da). Hence, water penetration can be expected to be faster than methylene blue penetration into the PLGA implants.

As it can be seen on the right hand side of Fig. 2, a shell of swollen PLGA is formed upon contact with the aqueous bulk fluid. Water is known to act as a plasticizer for PLGA (Passerini and Craig, 2001; Blasi et al., 2005). Consequently, the amorphous polymer "PLGA Resomer RG 502H" (50:50 lactic acid:glycolic acid) undergoes a glassy to rubbery phase transition (Faisant et al., 2002). Furthermore, the PLGA chains are initially relatively long and hydrophobic. Thus, water penetration into the system is limited at early time points: As it can be seen in Fig. 2 (right hand side), the thickness of the swollen PLGA shell increases only slowly: On day 3, most of the implant core is still non-swollen. This corresponds to a limited increase in the implants' wet weight during the first 3 d of exposure to the bulk fluid (blue curve in Fig. 3a). Importantly, afterwards the system takes up *substantial* amounts of water (Fig. 3a). This coincides with the disappearance of the non-swollen implant core and an important increase in system size (Fig. 2). A similar type of swelling behavior (lag time, followed by a substantial increase in the systems' wet weight) has recently also been reported for other types of HME implants, based on PLGA 50:50 (lactic acid:glycolic acid), PLGA 75:25 (lactic acid:glycolic acid) as well as on poly(lactic acid) (PLA) (Bode et al., 2019). A likely explanation for this behavior is the following: At early time points, the polymeric network is dense, highly entangled and hydrophobic. Thus, the amounts of water that can penetrate into the implants is limited. Nevertheless, small amounts of water can enter the system and start polymer degradation by ester bond cleavage throughout the device ("bulk erosion") (van Burkersroda et al., 2002). Consequently, the PLGA polymer molecular weight decreases. Since the newly created end groups are hydrophilic (–COOH and –OH), the polymer becomes more and more hydrophilic. In addition, the degree of polymer chain entanglement decreases and, thus, the mechanical resistance to substantial system swelling decreases. Also, water-soluble degradation products are generated, creating a steadily increasing osmotic pressure within the implants. As soon as the system is sufficiently hydrophilic and flexible (e.g. less entangled), implant swelling sets on. This starts at the implants' surface (since the water concentration is highest), but is limited until - after a certain lag time (here about 3 d) – the entire implant starts to substantially swell (Figs. 2 and 3a). The presence of a mechanically stable, non-swollen implant core can also be expected to avoid substantial entire implant swelling at early time points, due to steric hindrance. Once the entire implant started swelling, the water content of the system increases tremendously. These very high amounts of water allow the entrapped drug to dissolve and diffuse through the highly swollen system. Briefly, PLGA swelling plays an "orchestrating" role for the control of drug release, determining the onset of noteworthy drug dissolution and diffusion (Bode et al., 2019). The experimental results obtained in this study using methylene blue to stain the release medium confirm this theory: As it can be seen in Fig. 2, a drug can be expected to be able to dissolve and to be much more mobile in the highly swollen implant (e.g. after 7 d exposure) compared to the relatively dry and non-swollen implant cores during the first 3 d.

It has to be pointed out that the PLGA implants were surrounded by a liquid bulk fluid in this study, offering limited resistance to polymer swelling. In vivo, the mechanical properties of the environment are different. For instance, surrounding subcutaneous tissue can likely affect polymer swelling. Also, movements of the patient (e.g., muscle

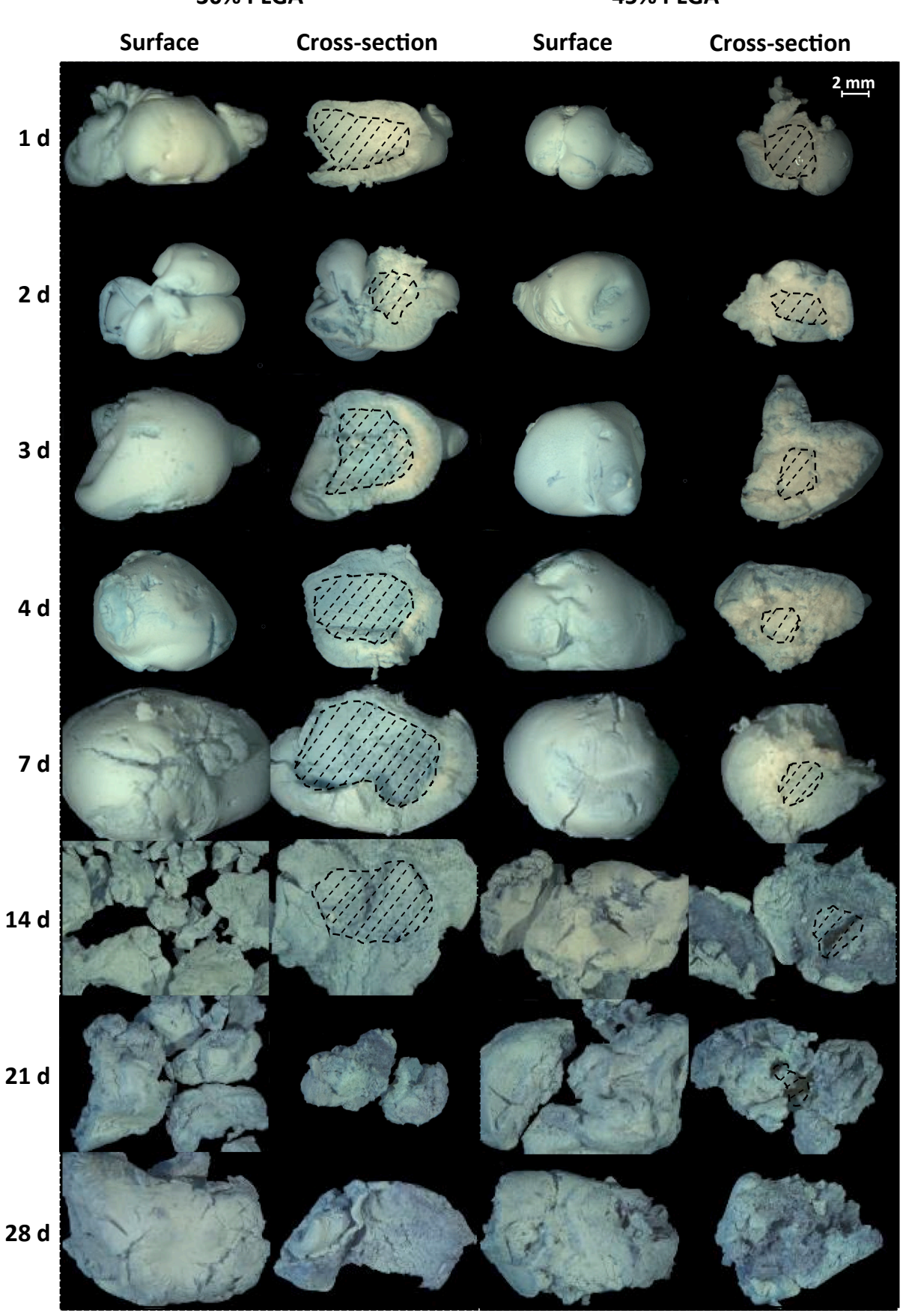

(caption on next page)

Fig. 6. Macroscopic pictures of (vitamin/dye-free) implants formed *in-situ* upon exposure to a 0.01% methylene blue solution in phosphate buffer pH 7.4, and subsequent freeze-drying. The time periods of exposure are indicated on the left hand side. Surfaces and cross-sections are shown. The liquid formulations contained 30 or 45% PLGA RG 502H (left and right hand side). (For interpretation of the references to color in this figure legend, the reader is referred to the web version of this article.)

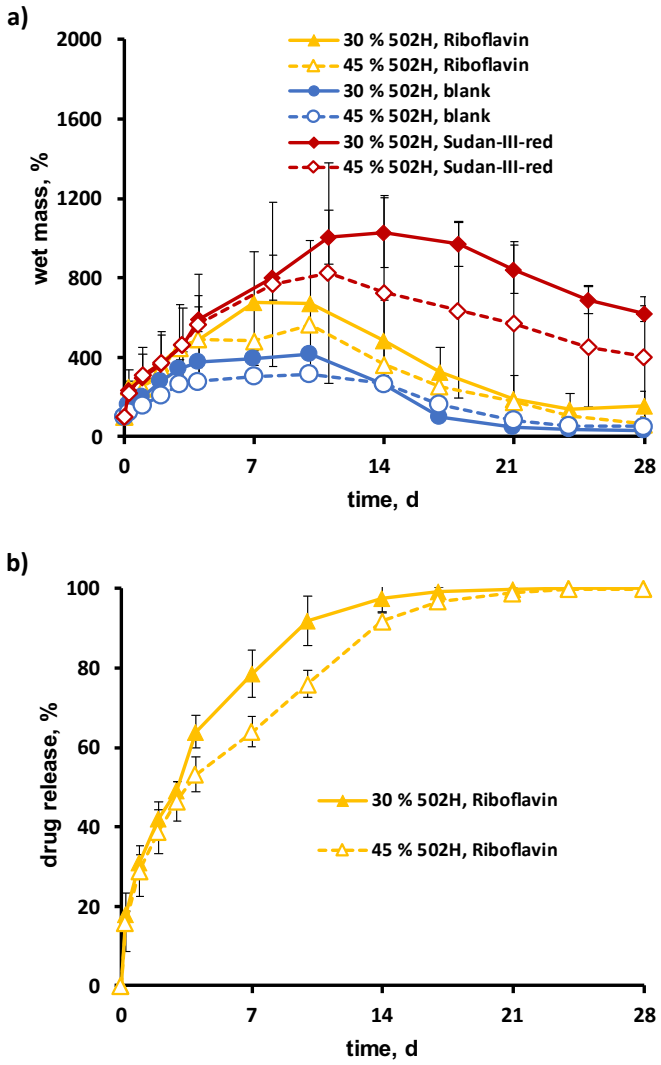

Fig. 7. a) Dynamic changes in the wet mass of *in-situ* forming implants: blank, or loaded with 1% riboflavin or Sudan-III-red (as indicated) upon exposure to aqueous bulk fluids. b) Riboflavin release from *in-situ* forming implants (1% vitamin loading) in phosphate buffer pH 7.4. The liquid formulations contained 30 or 45% PLGA RG 502H (as indicated). Mean values ± standard deviation are indicated (n = 3). (For interpretation of the references to color in this figure legend, the reader is referred to the web version of this article.)

contractions) probably deform highly swollen polymer regions. Yet, the impact of these phenomena on the resulting drug release kinetics is not fully understood. A very interesting study of Maeder et al. (1997) showed that plastic deformation of PLGA implants was observed in Wistar rats (upon s.c. administration in the neck, dorsal side) after a certain lag time, using Magnetic Resonance Imaging (MRI) analysis. The same type of implants behaved differently in vitro, when surrounded by a liquid bulk fluid. In the future, it will be interesting to study the impact of the in vivo conditions on PLGA swelling and drug release in more detail.

Note that the dark blue regions observed at later time points in Fig. 2 are likely artifacts created during freeze-drying: Probably, water-filled cavities are formed at these stages. Since methylene blue is water-soluble, it can be expected to be present in these cavities. Upon freeze-drying the water is removed, and the dye precipitates.

Fig. 4 shows macroscopic pictures of surfaces and cross-sections of PLGA HME implants, initially containing 1% riboflavin. This vitamin has a yellow color. The two pictures at the top illustrate the initial homogenous distribution of riboflavin throughout the implants, before exposure to the release medium. Upon contact with phosphate buffer pH 7.4, a swollen PLGA shell forms at the implants' surface, steadily growing. However, the water uptake during the first 3 d remains very limited (Fig. 3a), and a non-swollen core is clearly visible (as in the case of the blank implants exposed to an aqueous methylene blue solution). In this non-swollen implant core, the amount of water available for riboflavin dissolution is very limited and the mobility of dissolved vitamin molecules (or ions) can be expected to be very low. This is why riboflavin release is negligible during the first 3 d (Fig. 3b). But once the critical PLGA polymer molecular weight is reached, substantial amounts of water penetrate into the system (Fig. 3a), and the entire implant becomes highly hydrated (Fig. 4). Under these conditions, the vitamin can dissolve (solubility in phosphate buffer pH 7.4 at 37° C = 165.0 ± 1 μg/mL, but due to acidic micro-climates a much higher local solubility within the implants can be expected for this weak base). Once dissolved, the vitamin molecules/ions diffuse out of the system in the surrounding bulk fluid, due to concentration gradients. Note that after 7 d exposure to the bulk fluid, the inner parts of the implants were still dark yellow (Fig. 4, right hand side), whereas the outer regions were bright yellow. This nicely illustrates the vitamin concentration gradients within the systems (which are the driving forces for diffusion).

In addition, Sudan-III-red was used to color HME implants: a poorly water-soluble, lipophilic dye. The two pictures at the top of Fig. 5 show the homogenous initial distribution of this compound in the PLGA implants prior to exposure to the aqueous bulk fluid. In this case, 0.02% Tween 80 was added to the phosphate buffer, to allow for complete dye release within several weeks under the given experimental conditions. Note that the presence of this surfactant might alter the velocity of some of the involved mass transport processes to a certain extent (e.g. water penetration into the system). However, this potential impact is likely limited, as indicated by the following observations: Analogous to the blank and riboflavin-loaded HME implants (Figs. 2–4), during the first 3 d, a swollen polymer shell formed at the cylinders' surface, while the systems' core remained non-swollen. Again, after this lag time, substantial implant swelling set on (Fig. 3a), allowing for Sudan-III-red release into the surrounding bulk fluid. As in the case of riboflavin, vitamin/dye concentration gradients from the core in the direction of the surfaces of the implants were observed, e.g. after 7 d. Thus, also in this case, the "orchestrating" role of PLGA swelling for the control of drug/vitamin/dye release from HME implants could be confirmed visually.

3.2. *In-situ forming implants*

Fig. 6 shows pictures of surfaces and cross-sections of blank PLGA implants that formed *in-situ*, upon injection of a solution of "Resomer RG 502H" in N-methyl-pyrrolidone (NMP) into phosphate buffer pH 7.4 containing 0.01% methylene blue (37 °C). The polymer concentration in the NMP solution was 30 or 45% (left and right hand side), respectively. At pre-determined time points, the implants were withdrawn from the bulk fluid and freeze-dried. Again, note that this drying process created artifacts. The cross-sections were obtained by manual breaking, the dashed curves indicate the presence of hollow cavities in the freeze-dried implants. Clearly, cavities were formed at the center of

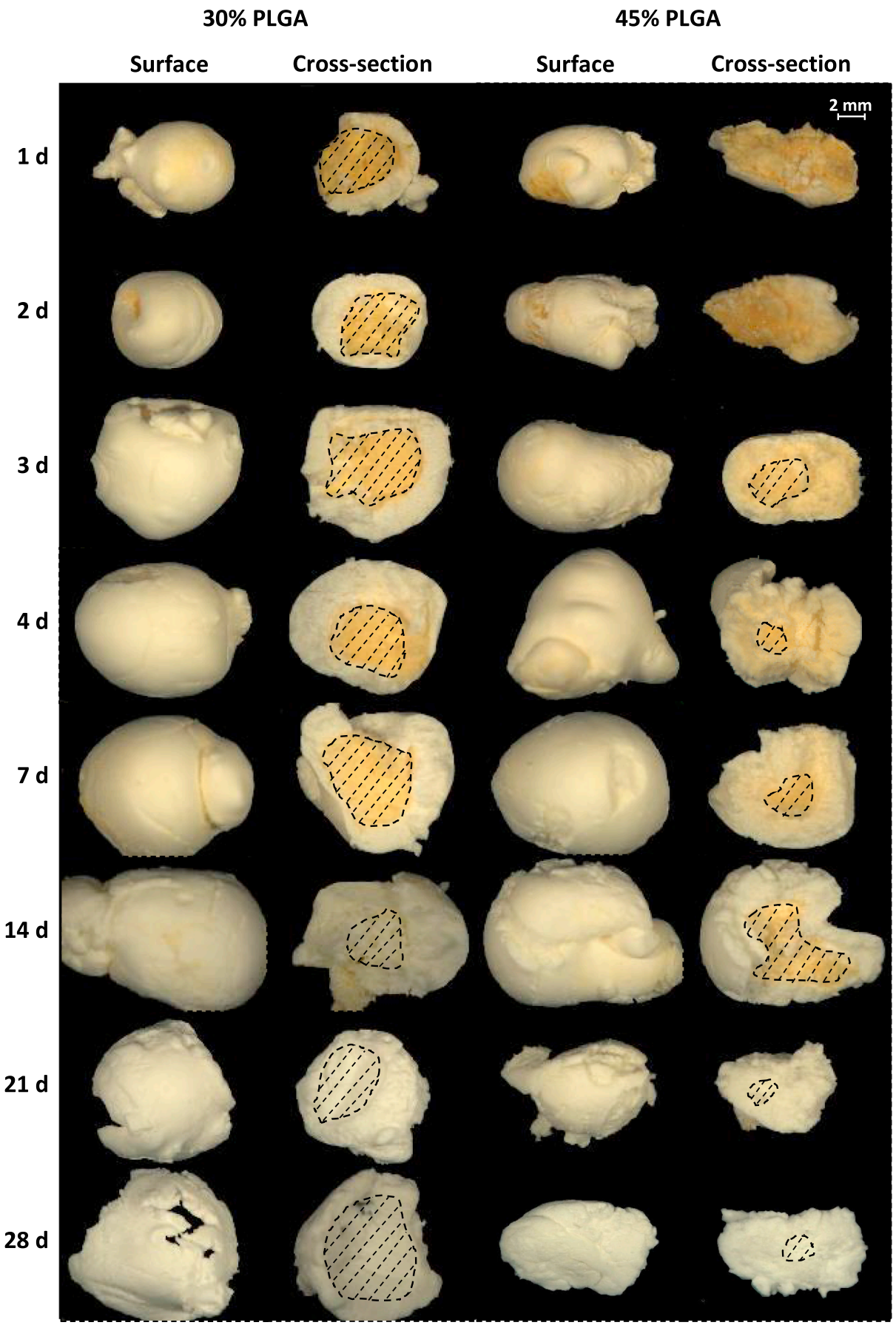

(caption on next page)

Fig. 8. Macroscopic pictures of implants loaded with 1% riboflavin formed *in-situ* upon exposure to phosphate buffer pH 7.4, and subsequent freeze-drying. The time periods of exposure are indicated on the left hand side. Surfaces and cross-sections are shown. The liquid formulations contained 30 or 45% PLGA RG 502H (left and right hand side).

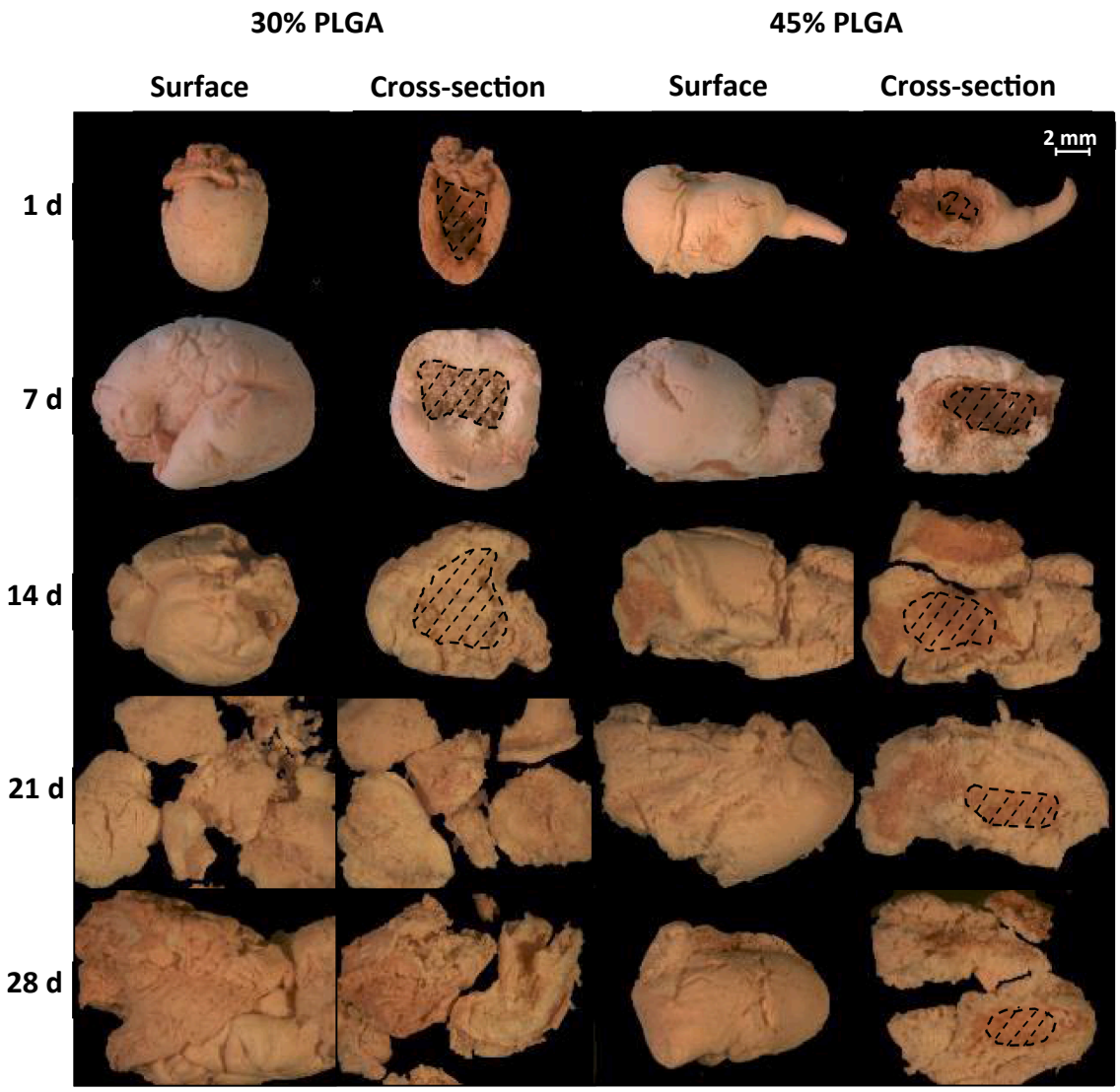

Fig. 9. Macroscopic pictures of implants loaded with 1% Sudan-III-red formed *in-situ* upon exposure to phosphate buffer pH 7.4, and subsequent freeze-drying. The time periods of exposure are indicated on the left hand side. Surfaces and cross-sections are shown. The liquid formulations contained 30 or 45% PLGA RG 502H (left and right hand side). (For interpretation of the references to color in this figure legend, the reader is referred to the web version of this article.)

the implants, irrespective of the polymer concentration in the liquid formulations. This can be explained as follows: Initially, the PLGA is dissolved in the NMP. Upon contact with the aqueous phosphate buffer solution, water diffuses into the NMP formulation and NMP diffuses into the aqueous bulk fluid (water and NMP being miscible). Consequently, the solubility of the PLGA in the formulation decreases (not being soluble in water). The decrease in polymer solubility is most important at the interface "formulation – aqueous bulk fluid", since the water content is highest and the NMP content lowest. Consequently, a PLGA shell forms at this interface (Bode et al., 2018). This shell grows inwards: in the direction of the core of the *in-situ* forming implant. At a certain time point, all PLGA has precipitated and a hollow center remains (the amount of polymer in the formulation is insufficient to entirely fill the implant). The central cavity is initially mainly filled with NMP/water mixtures, later mainly with water (in which short chain polymer degradation products, buffer salts and methylene blue are dissolved). At a PLGA content of 45% in the liquid NMP formulation, more polymer is available to fill the implant compared to the formulations containing only 30% PLGA. Consequently, the PLGA "walls" of the respective implants are thicker (pictures on the right hand side in Fig. 6 compared to pictures on the left hand side). One of the consequences of the thicker implant walls is a lower water penetration rate into the system (dashed vs. solid blue curve in Fig. 7a). Another consequence is a slower methylene blue penetration into the thicker PLGA walls of implants prepared with 45 compared to 30% polymer content (cross-sections in Fig. 6). [Again, note that water can be expected to be more mobile than the dye, due to the difference in molecular weight]. It has previously been shown that the thicker PLGA implant walls resulting from higher polymer concentrations also lead to more pronounced autocatalytic effects and accelerated PLGA degradation (Bode et al., 2018).

Surfaces and cross-section of *in-situ* formed implants loaded with 1% riboflavin (referred to 100% = vitamin + PLGA + NMP) are shown in Fig. 8. The PLGA content of the NMP solution was 30 and 45% (left and

right hand side). Again, a clear difference in implant wall thickness was observed, confirming the above described hypotheses. Furthermore, the implants' central cavities were initially dark yellow, because the water (at early time points also NMP) was removed during freeze-drying, leading to artificial riboflavin precipitation. The thicker PLGA walls also slowed down vitamin release: As it can be seen in Fig. 7b, riboflavin release was slower at 45% polymer content of the NMP formulation compared to 30%. This is also consistent with the cross-sections overserved after 14 d (Fig. 8, difference in the intensity of the yellow color in the implants), and with the reduced water uptake rates and extents of the implants at higher PLGA concentrations (dashed vs. solid yellow curves in Fig. 7a).

These tendencies were further confirmed with *in-situ* forming implants loaded with Sudan-III-red: Fig. 9 shows surfaces and cross-sections of implants formed upon injection of a solution of PLGA (30 or 45%) and dye (1%) in NMP into phosphate buffer pH 7.4 (containing 0.02% Tween 80 to facilitate the release of this poorly water-soluble dye under the given experimental conditions). The thicker implants walls obtained with formulations containing 45% PLGA slowed down dye release, as indicated by the red color remaining for longer time periods within these implants compared to systems obtained with formulations containing only 30% PLGA. Again, the thicker walls also reduced the extent and the rate at which water penetrated into the implants (dashed vs. solid red curves in Fig. 7a).

Thus, in all cases, the use of dyes in the formulations or in the release medium as well as the use of a colored vitamin could help visualizing the mechanisms of *in-situ* implant formation and help to better understand the impact of the composition of the liquid formulations on the key properties of the implants, including their swelling and release behavior.

4. Conclusion

The results obtained in this study with dyes and a colored vitamin allowed getting further insight into the mechanisms controlling drug release from PLGA-based implants. In the case of pre-formed, hot melt extruded implants, the orchestrating role of PLGA swelling for the control of drug release could be visualized. In the case of *in-situ* forming implants based on solvent exchange, the impact of the liquid formulation's composition on the systems' key properties could be better understood. This knowledge can help facilitating: (i) the optimization of PLGA-based implants (and most likely also of other biodegradable controlled release dosage forms), and (ii) the explanation of sometimes surprising tendencies observed with PLGA-based drug delivery systems in vitro and in vivo.

Declaration of Competing Interest

The authors declare the following financial interests/personal relationships which may be considered as potential competing interests: The Editor-in-Chief of the journal is one of the co-authors of this article. The manuscript has been subject to all of the journal's usual procedures, including peer review, which has been handled independently of the Editor-in-Chief.

Appendix A. Supplementary data

Supplementary data to this article can be found online at https://doi.org/10.1016/j.ijpharm.2019.118563.

References

Agossa, K., Lizambard, M., Rongthong, T., Delcourt-Debruyne, E., Siepmann, J., Siepmann, F., 2017. Physical key properties of antibiotic-free, PLGA/HPMC-based in-situ forming implants for local periodontitis treatment. Int. J. Pharmaceut. 521, 282–293. https://doi.org/10.1016/j.ijpharm.2017.02.039.

Anderson, J.M., Shive, M.S., 1997. Biodegradation and biocompatibility of PLA and PLGA microspheres. Adv. Drug Deliv. Rev Biodegrad. Microspheres/Ther. Peptide Deliv. 28, 5–24. https://doi.org/10.1016/S0169-409X(97)00048-3.

Astaneh, R., Erfan, M., Barzin, J., Mobedi, H., Moghimi, H., 2008. Effects of ethyl benzoate on performance, morphology, and erosion of PLGA implants formed in situ. Adv. Polym. Tech. 27, 17–26. https://doi.org/10.1002/adv.20114.

Berkland, C., King, M., Cox, A., Kim, K., Pack, D.W., 2002. Precise control of PLG microsphere size provides enhanced control of drug release rate. J. Control. Release 82, 137–147. https://doi.org/10.1016/S0168-3659(02)00136-0.

Berkland, C., Pollauf, E., Raman, C., Silverman, R., Kim, K., Pack, D.W., 2007. Macromolecule Release from Monodisperse PLG Microspheres: Control of Release Rates and Investigation of Release Mechanism. J. Pharm. Sci. 96, 1176–1191. https://doi.org/10.1002/jps.20948.

Blasi, P., D'Souza, S.S., Selmin, F., DeLuca, P.P., 2005. Plasticizing effect of water on poly (lactide-co-glycolide). J. Control. Release 108, 1–9. https://doi.org/10.1016/j.jconrel.2005.07.009.

Bode, C., Kranz, H., Siepmann, F., Siepmann, J., 2018. In-situ forming PLGA implants for intraocular dexamethasone delivery. Int. J. Pharmaceut. 548, 337–348. https://doi.org/10.1016/j.ijpharm.2018.07.013.

Bode, C., Kranz, H., Siepmann, F., Siepmann, J., 2019. Often neglected: PLGA/PLA swelling orchestrates drug release - HME implants. J. Control. Release 306, 97–107. https://doi.org/10.1016/j.jconrel.2019.05.039.

Bragagni, M., Gil-Alegre, M.E., Mura, P., Cirri, M., Ghelardini, C., Di Cesare Mannelli, L., 2018. Improving the therapeutic efficacy of prilocaine by PLGA microparticles: Preparation, characterization and in vivo evaluation. Int. J. Pharmaceut. 547, 24–30. https://doi.org/10.1016/j.ijpharm.2018.05.054.

Brunner, A., Mäder, K., Göpferich, A., 1999. pH and osmotic pressure inside biodegradable microspheres during erosion1. Pharm. Res. 16, 847–853. https://doi.org/10.1023/A:1018822002353.

DesNoyer, J.R., McHugh, A.J., 2003. The effect of Pluronic on the protein release kinetics of an injectable drug delivery system. J. Control. Release 86, 15–24. https://doi.org/10.1016/S0168-3659(02)00293-6.

Do, M.P., Neut, C., Delcourt, E., Seixas Certo, T., Siepmann, J., Siepmann, F., 2014. In situ forming implants for periodontitis treatment with improved adhesive properties. Eur. J. Pharm. Biopharm. 88, 342–350. https://doi.org/10.1016/j.ejpb.2014.05.006.

Do, M.P., Neut, C., Metz, H., Delcourt, E., Mäder, K., Siepmann, J., Siepmann, F., 2015a. In-situ forming composite implants for periodontitis treatment: How the formulation determines system performance. Int. J. Pharmaceut. 486, 38–51. https://doi.org/10.1016/j.ijpharm.2015.03.026.

Do, M.P., Neut, C., Metz, H., Delcourt, E., Siepmann, J., Mäder, K., Siepmann, F., 2015b. Mechanistic analysis of PLGA/HPMC-based in-situ forming implants for periodontitis treatment. Eur. J. Pharm. Biopharm. 94, 273–283. https://doi.org/10.1016/j.ejpb.2015.05.018.

Duque, L., Körber, M., Bodmeier, R., 2018. Improving release completeness from PLGA-based implants for the acid-labile model protein ovalbumin. Int. J. Pharmaceut. 538, 139–146. https://doi.org/10.1016/j.ijpharm.2018.01.026.

Faisant, N., Siepmann, J., Benoit, J.P., 2002. PLGA-based microparticles: elucidation of mechanisms and a new, simple mathematical model quantifying drug release. Eur. J. Pharm. Sci. 15, 355–366. https://doi.org/10.1016/S0928-0987(02)00023-4.

Fournier, E., Passirani, C., Montero-Menei, C.N., Benoit, J.P., 2003. Biocompatibility of implantable synthetic polymeric drug carriers: focus on brain biocompatibility. Biomaterials 24, 3311–3331. https://doi.org/10.1016/S0142-9612(03)00161-3.

Fredenberg, S., Jönsson, M., Laakso, T., Wahlgren, M., Reslow, M., Axelsson, A., 2011. Development of mass transport resistance in poly(lactide-co-glycolide) films and particles – A mechanistic study. Int. J. Pharmaceut. 409, 194–202. https://doi.org/10.1016/j.ijpharm.2011.02.066.

Friess, W., Schlapp, M., 2002. Release mechanisms from gentamicin loaded poly(lactic-co-glycolic acid) (PLGA) microparticles. J. Pharm. Sci. 91, 845–855. https://doi.org/10.1002/jps.10012.

Fu, K., Pack, D.W., Klibanov, A.M., Langer, R., 2000. Visual evidence of acidic environment within degrading poly(lactic-co-glycolic acid) (PLGA) microspheres. Pharm. Res. 17, 100–106.

Gasmi, H., Danede, F., Siepmann, J., Siepmann, F., 2015a. Does PLGA microparticle swelling control drug release? New insight based on single particle swelling studies. J. Control. Release 213, 120–127. https://doi.org/10.1016/j.jconrel.2015.06.039.

Gasmi, H., Willart, J.-F., Danede, F., Hamoudi, M.C., Siepmann, J., Siepmann, F., 2015b. Importance of PLGA microparticle swelling for the control of prilocaine release. J. Drug Deliv. Sci. Technol. 30, 123–132. https://doi.org/10.1016/j.jddst.2015.10.009.

Gasmi, H., Siepmann, F., Hamoudi, M.C., Danede, F., Verin, J., Willart, J.-F., Siepmann, J., 2016. Towards a better understanding of the different release phases from PLGA microparticles: Dexamethasone-loaded systems. Int. J. Pharmaceut., In Honour of Professor Alexander T. FlorenceIn Honour of Professor Alexander T. Florence 514, 189–199. https://doi.org/10.1016/j.ijpharm.2016.08.032.

Ghalanbor, Z., Körber, M., Bodmeier, R., 2012. Protein release from poly(lactide-co-glycolide) implants prepared by hot-melt extrusion: Thioester formation as a reason for incomplete release. Int. J. Pharmaceut. 438, 302–306. https://doi.org/10.1016/j.ijpharm.2012.09.015.

Gilding, D.K., Reed, A.M., 1979. Biodegradable polymers for use in surgery—polyglycolic/poly(actic acid) homo- and copolymers: 1. Polymer 20, 1459–1464. https://doi.org/10.1016/0032-3861(79)90009-0.

Gonzalez-Pizarro, R., Silva-Abreu, M., Calpena, A.C., Egea, M.A., Espina, M., García, M.L., 2018. Development of fluorometholone-loaded PLGA nanoparticles for treatment of inflammatory disorders of anterior and posterior segments of the eye. Int. J. Pharmaceut. 547, 338–346. https://doi.org/10.1016/j.ijpharm.2018.05.050.

Gopferich, A., 1996. Polymer degradation and erosion: Mechanisms and applications. Eur. J. Pharm. Biopharm. 42, 1–11.

Hamoudi-Ben Yelles, M.C., Tran Tan, V., Danede, F., Willart, J.F., Siepmann, J., 2017. PLGA implants: How Poloxamer/PEO addition slows down or accelerates polymer degradation and drug release. J. Control. Release 253, 19–29. https://doi.org/10.1016/j.jconrel.2017.03.009.

Hatefi, A., Amsden, B., 2002. Biodegradable injectable in situ forming drug delivery systems. J. Control. Release 80, 9–28. https://doi.org/10.1016/S0168-3659(02)00008-1.

Ibrahim, M.A., Ismail, A., Fetouh, M.I., Göpferich, A., 2005. Stability of insulin during the erosion of poly(lactic acid) and poly(lactic-co-glycolic acid) microspheres. J. Control. Release 106, 241–252. https://doi.org/10.1016/j.jconrel.2005.02.025.

Johansen, P., Corradin, G., Merkle, H.P., Gander, B., 1998. Release of tetanus toxoid from adjuvants and PLGA microspheres: How experimental set-up and surface adsorption fool the pattern. J. Control. Release 56, 209–217. https://doi.org/10.1016/S0168-3659(98)00084-4.

Kamali, H., Khodaverdi, E., Hadizadeh, F., Yazdian-Robati, R., Haghbin, A., Zohuri, G., 2018. An in-situ forming implant formulation of naltrexone with minimum initial burst release using mixture of PLGA copolymers and ethyl heptanoate as an additive: In-vitro, ex-vivo, and in-vivo release evaluation. J. Drug Deliv. Sci. Technol. 47, 95–105. https://doi.org/10.1016/j.jddst.2018.06.027.

Kang, J., Schwendeman, S.P., 2007. Pore closing and opening in biodegradable polymers and their effect on the controlled release of proteins. Mol. Pharm. 4, 104–118. https://doi.org/10.1021/mp060041n.

Kempe, S., Mäder, K., 2012. In situ forming implants — an attractive formulation principle for parenteral depot formulations. J. Controlled Release, Drug Deliv. Res. Europe 161, 668–679. https://doi.org/10.1016/j.jconrel.2012.04.016.

Kempe, S., Metz, H., Mäder, K., 2008. Do in situ forming PLG/NMP implants behave similar in vitro and in vivo? A non-invasive and quantitative EPR investigation on the mechanisms of the implant formation process. J. Control. Release 130, 220–225. https://doi.org/10.1016/j.jconrel.2008.06.006.

Klose, D., Siepmann, F., Elkharraz, K., Krenzlin, S., Siepmann, J., 2006. How porosity and size affect the drug release mechanisms from PLGA-based microparticles. Local Controlled Drug Delivery to the Brain. Int. J. Pharmaceut. 314, 198–206. https://doi.org/10.1016/j.ijpharm.2005.07.031.

Klose, D., Siepmann, F., Elkharraz, K., Siepmann, J., 2008. PLGA-based drug delivery systems: Importance of the type of drug and device geometry. Special Issue in Honor of Prof. Tsuneji Nagai. Int. J. Pharmaceut. 354, 95–103. https://doi.org/10.1016/j.ijpharm.2007.10.030.

Kranz, H., Bodmeier, R., 2007. A novel in situ forming drug delivery system for controlled parenteral drug delivery. Int. J. Pharmaceut. 332, 107–114. https://doi.org/10.1016/j.ijpharm.2006.09.033.

Kranz, H., Bodmeier, R., 2008. Structure formation and characterization of injectable drug loaded biodegradable devices: In situ implants versus in situ microparticles. Eur. J. Pharm. Sci. 34, 164–172. https://doi.org/10.1016/j.ejps.2008.03.004.

Lee, S.S., Hughes, P., Ross, A.D., Robinson, M.R., 2010. Biodegradable Implants for Sustained Drug Release in the Eye. Pharm. Res. 27, 2043–2053. https://doi.org/10.1007/s11095-010-0159-x.

Lin, X., Yang, H., Su, L., Yang, Z., Tang, X., 2018. Effect of size on the in vitro/in vivo drug release and degradation of exenatide-loaded PLGA microspheres. J. Drug Deliv. Sci. Technol. 45, 346–356. https://doi.org/10.1016/j.jddst.2018.03.024.

Maeder, K., Bacic, G., Domb, A., Elmalak, O., Langer, R., Swartz, H.M., 1997. Noninvasive in vivo monitoring of drug release and polymer erosion from biodegradable polymers by EPR spectroscopy and NMR imaging. J. Pharm. Sci. 86, 126–134. https://doi.org/10.1021/js9505105.

Mylonaki, I., Allémann, E., Delie, F., Jordan, O., 2018a. Imaging the porous structure in the core of degrading PLGA microparticles: The effect of molecular weight. J. Control. Release 286, 231–239. https://doi.org/10.1016/j.jconrel.2018.07.044.

Mylonaki, I., Trosi, O., Allémann, E., Durand, M., Jordan, O., Delie, F., 2018b. Design and characterization of a perivascular PLGA coated PET mesh sustaining the release of atorvastatin for the prevention of intimal hyperplasia. Int. J. Pharmaceut. 537, 40–47. https://doi.org/10.1016/j.ijpharm.2017.12.026.

Passerini, N., Craig, D.Q.M., 2001. An investigation into the effects of residual water on the glass transition temperature of polylactide microspheres using modulated temperature DSC. J. Control. Release 73, 111–115. https://doi.org/10.1016/S0168-3659(01)00245-0.

Ravivarapu, H.B., Burton, K., DeLuca, P.P., 2000. Polymer and microsphere blending to alter the release of a peptide from PLGA microspheres. Eur. J. Pharm. Biopharm. 50, 263–270. https://doi.org/10.1016/S0939-6411(00)00099-0.

Schädlich, A., Kempe, S., Mäder, K., 2014. Non-invasive in vivo characterization of microclimate pH inside in situ forming PLGA implants using multispectral fluorescence imaging. J. Control. Release 179, 52–62. https://doi.org/10.1016/j.jconrel.2014.01.024.

Shah, R.B., Schwendeman, S.P., 2014. A biomimetic approach to active self-microencapsulation of proteins in PLGA. J. Control. Release 196, 60–70. https://doi.org/10.1016/j.jconrel.2014.08.029.

Sheikh Hasan, A., Sapin, A., Damgé, C., Leroy, P., Socha, M., Maincent, P., 2015. Reduction of the in vivo burst release of insulin-loaded microparticles. Honor of Prof. Dominique Duchêne. J. Drug Deliv. Sci. Technol. 30, 486–493. https://doi.org/10.1016/j.jddst.2015.06.020.

Siepmann, J., Siepmann, F., 2012. Modeling of diffusion controlled drug delivery. J. Controlled ReleaseDrug Deliv. Res. Eur. 161, 351–362. https://doi.org/10.1016/j.jconrel.2011.10.006.

Siepmann, J., Siepmann, F., 2013. Mathematical modeling of drug dissolution. Int. J. Pharmaceut. Poorly Soluble Drugs 453, 12–24. https://doi.org/10.1016/j.ijpharm.2013.04.044.

Siepmann, J., Elkharraz, K., Siepmann, F., Klose, D., 2005. How autocatalysis accelerates drug release from PLGA-based microparticles: a quantitative treatment. Biomacromolecules 6, 2312–2319. https://doi.org/10.1021/bm050228k.

Vert, M., Mauduit, J., Li, S., 1994. Biodegradation of PLA/GA polymers: increasing complexity. Biomaterials 15, 1209–1213. https://doi.org/10.1016/0142-9612(94)90271-2.

von Burkersroda, F., Schedl, L., Göpferich, A., 2002. Why degradable polymers undergo surface erosion or bulk erosion. Biomaterials 23, 4221–4231. https://doi.org/10.1016/S0142-9612(02)00170-9.

Wang, L., Kleiner, L., Venkatraman, S., 2003. Structure formation in injectable poly (lactide–co-glycolide) depots. J. Control. Release 90, 345–354. https://doi.org/10.1016/S0168-3659(03)00198-6.

Wischke, C., Schwendeman, S.P., 2008. Principles of encapsulating hydrophobic drugs in PLA/PLGA microparticles. Future Perspectives in Pharmaceutics Contributions from Younger Scientists. Int. J. Pharmaceut. 364, 298–327. https://doi.org/10.1016/j.ijpharm.2008.04.042.

Wischke, C., Schwendeman, S.P., 2012. Degradable polymeric carriers for parenteral controlled drug delivery. In: Siepmann, J., Siegel, R.A., Rathbone, M.J. (Eds.), Fundamentals and Applications of Controlled Release Drug Delivery, Advances in Delivery Science and Technology. Technology. Springer, US, Boston, MA, pp. 171–228. https://doi.org/10.1007/978-1-4614-0881-9_8.

Wu, C., Baldursdottir, S., Yang, M., Mu, H., 2018. Lipid and PLGA hybrid microparticles as carriers for protein delivery. J. Drug Deliv. Sci. Technol. 43, 65–72. https://doi.org/10.1016/j.jddst.2017.09.006.

Zhang, Y., Schwendeman, S.P., 2012. Minimizing acylation of peptides in PLGA microspheres. J. Control. Release 162, 119–126. https://doi.org/10.1016/j.jconrel.2012.04.022.